Electronic Supplementary Material (ESI) for Inorganic Chemistry Frontiers.

Electronic supplementary information

Copper molybdenum sulfide nanoparticles embedded on graphene sheets as advanced electrode for wide temperature-tolerant supercapacitor

Surjit Sahoo[a], Karthikeyan Krishnamoorthy[a], Parthiban Pazhamalai[a],

Vimal Kumar Mariappan[a] and Sang Jae Kim[a,b*]

[a] Nanomaterials and System Lab, Department of Mechatronics Engineering, Jeju National University, Jeju 63243, South Korea.

[b] Department of Advanced Convergence Science and Technology, Jeju National University, Jeju 63243, South Korea.

*Corresponding author. Email: kimsangj@jejunu.ac.kr

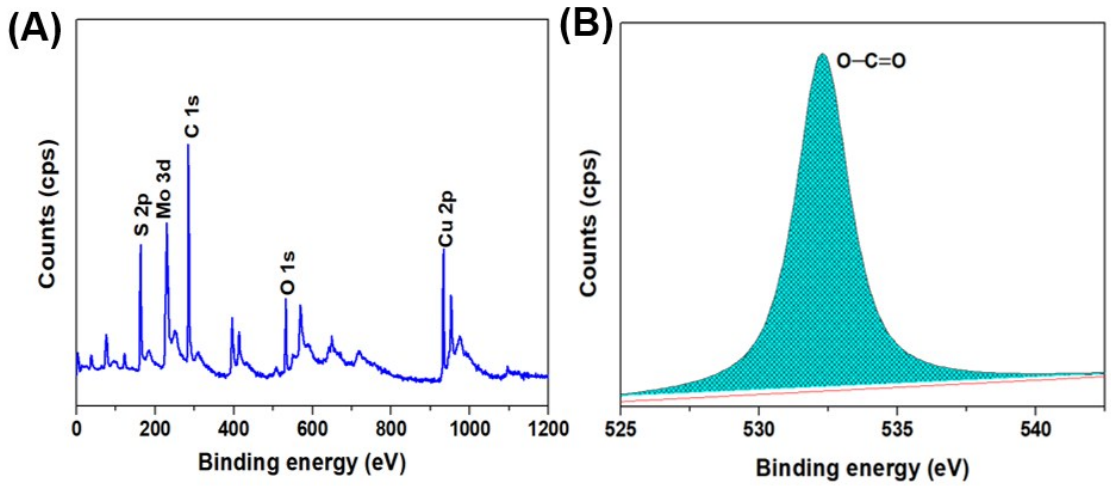

Figure S1. High resolution X-ray photoelectron spectrum (XPS) of as prepared Cu_2MoS_4-rGO hybrid (A) Survey spectrum in the range of 0 to 1200 eV, and (B) core level spectrum of O 1s state.

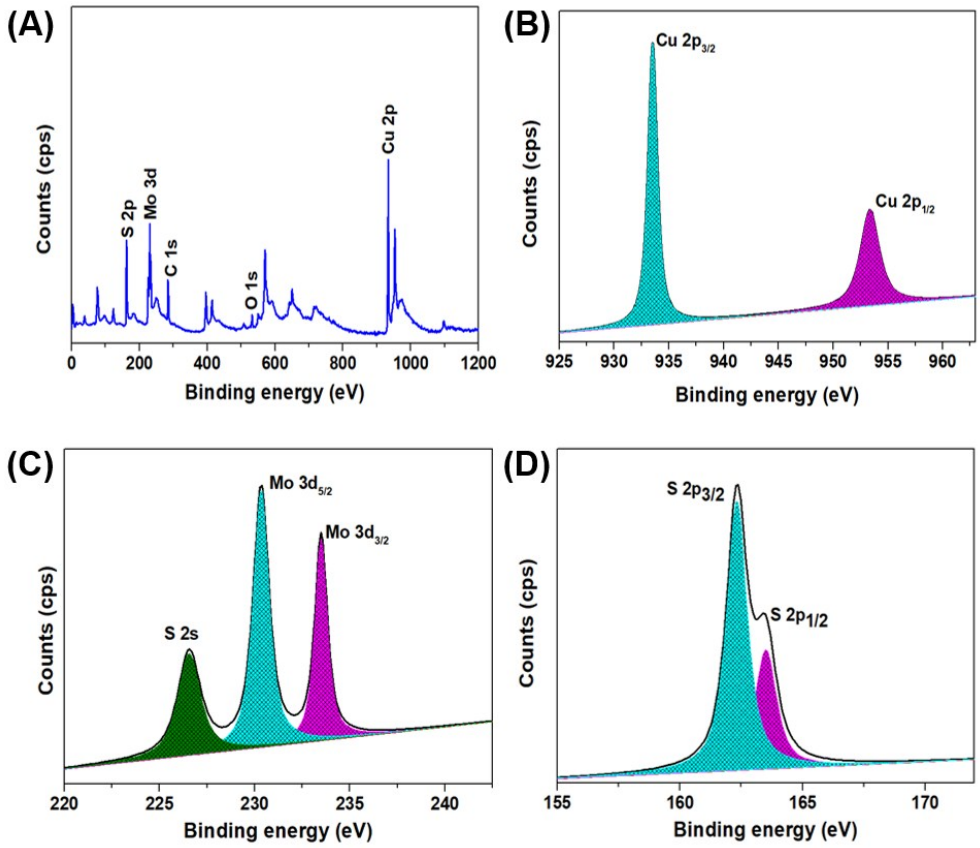

Figure S2. High resolution X-ray photoelectron spectrum (XPS) of as prepared Cu_2MoS_4 (A) Survey spectrum in the range of 0 to 1200 eV, (B) core level spectrum of Cu 2p state, (C) core level spectrum of Mo 3d state, (D) core level spectrum of S 2p state.

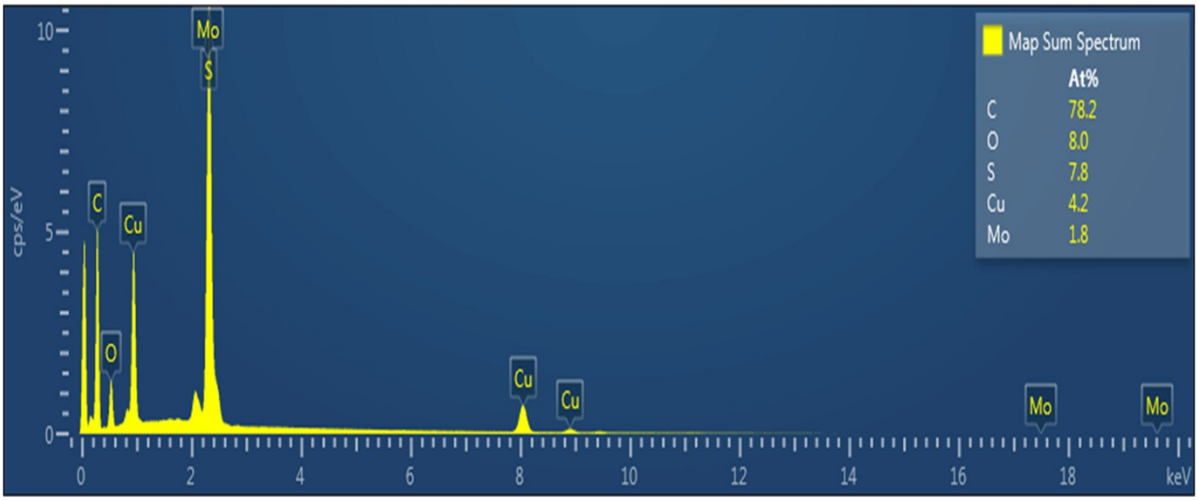

Figure S3. (A) Energy dispersive X-ray spectroscopic (EDS) analysis of Cu_2MoS_4-rGO hybrid.

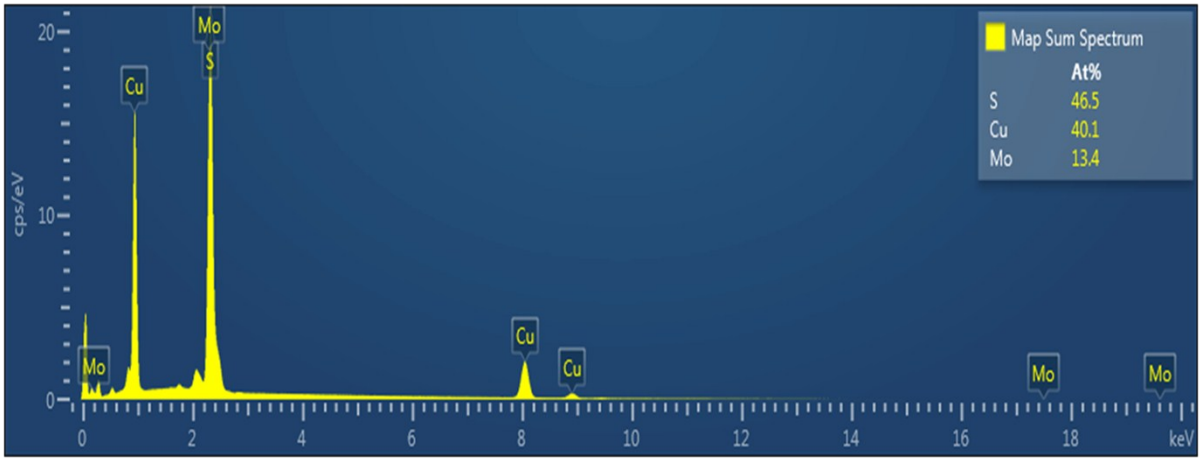

Figure S4. (A) Energy dispersive X-ray spectroscopic (EDS) analysis of as prepared Cu_2MoS_4.

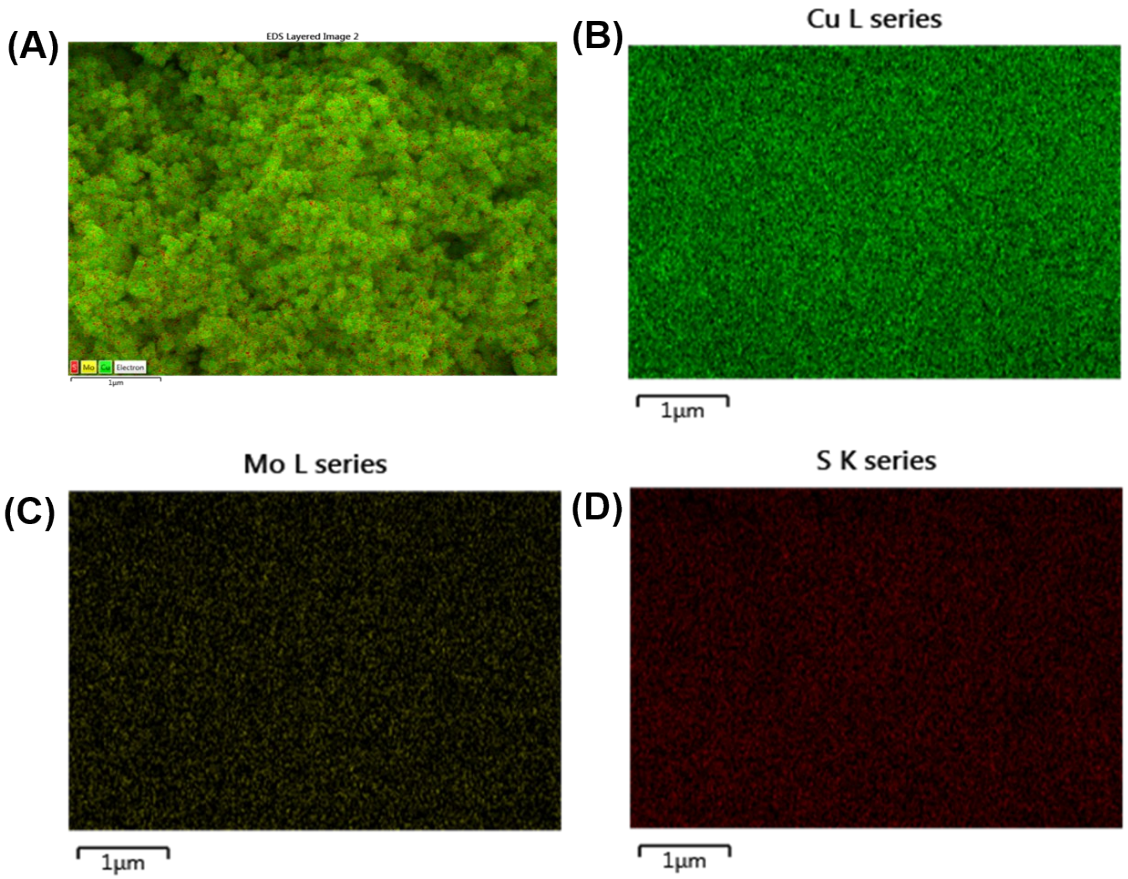

Figure S5. Elemental mapping of as prepared Cu_2MoS_4 (A) FE-SEM micrographs for elemental mapping, (B) copper, (C) molybdenum, (D) sulfur.

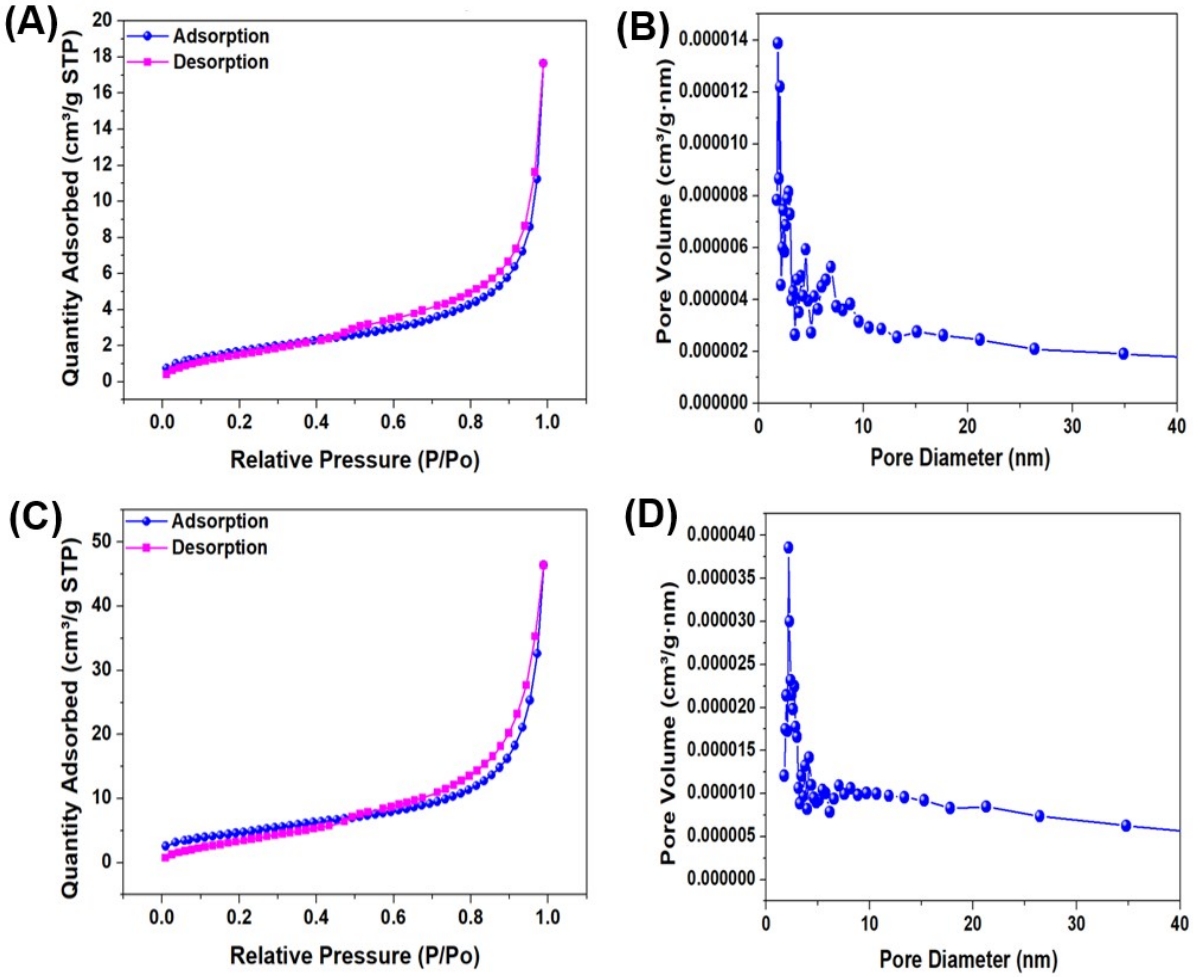

Figure S6. The Brunauer-Emmett-Teller (BET) and the Barrett-Joyner Halenda (BJH) analysis of pristine Cu_2MoS_4 and Cu_2MoS_4-rGO hybrid: (A) N_2 adsorption-desorption isotherms of pristine Cu_2MoS_4, (B) pore size distribution curve pristine Cu_2MoS_4, (C) N_2 adsorption-desorption isotherms of Cu_2MoS_4-rGO hybrid, and (D) pore size distribution curve of Cu_2MoS_4-rGO hybrid.

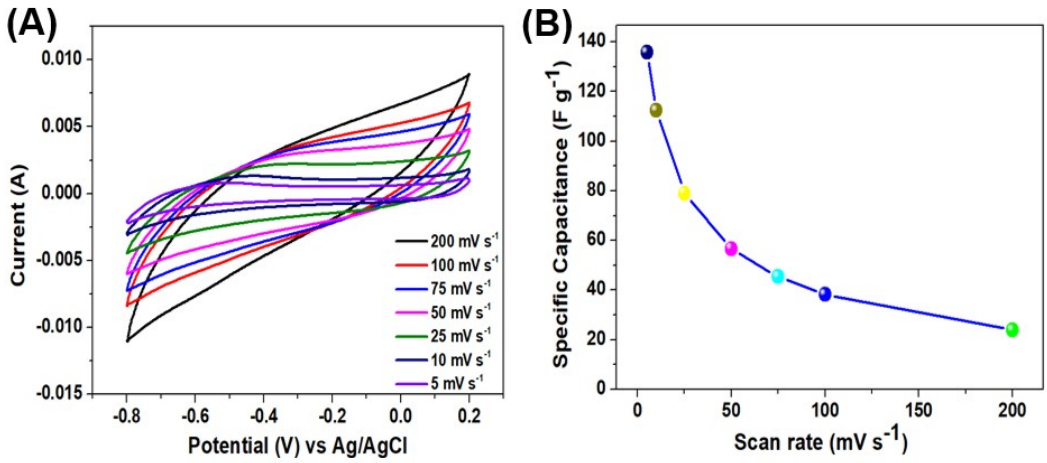

Figure S7. Electrochemical performance of as prepared Cu_2MoS_4 electrode, (A) cyclic voltammetric profile of the Cu_2MoS_4 electrode at various scan rates (5 to 200 mV s^{-1}), and (B) effect of scan rate on the specific capacitance of Cu_2MoS_4 electrode.

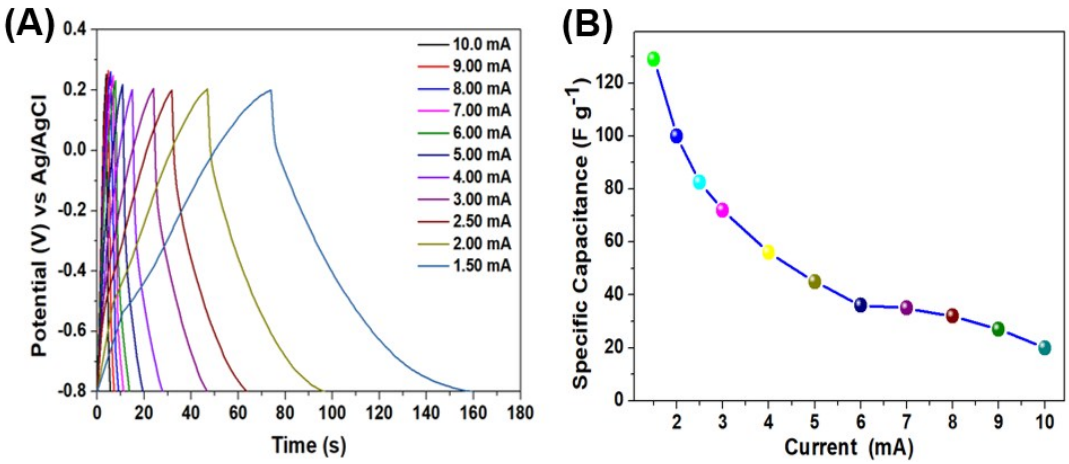

Figure S8. Electrochemical performance of as prepared Cu_2MoS_4 electrode, (A) Galvanostatic charge-discharge profile of Cu_2MoS_4 electrode measured at different current (1.5 to 10 mA) and (F) effect of current on the specific capacitance of Cu_2MoS_4 electrode.

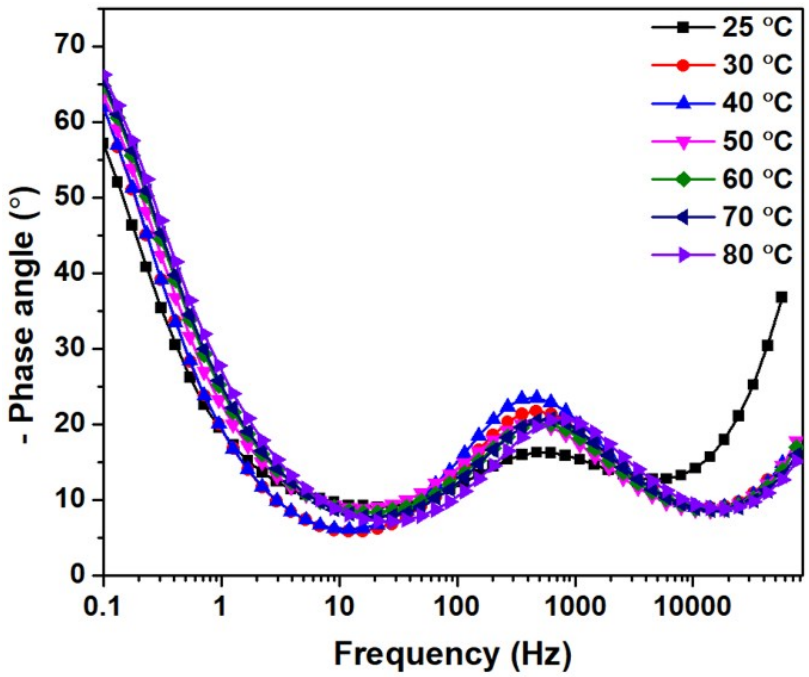

Figure S9. Variation of Bode phase angle concerning frequency of Cu_2MoS_4-rGO electrode at different operating temperature (25 °C to 80 °C).

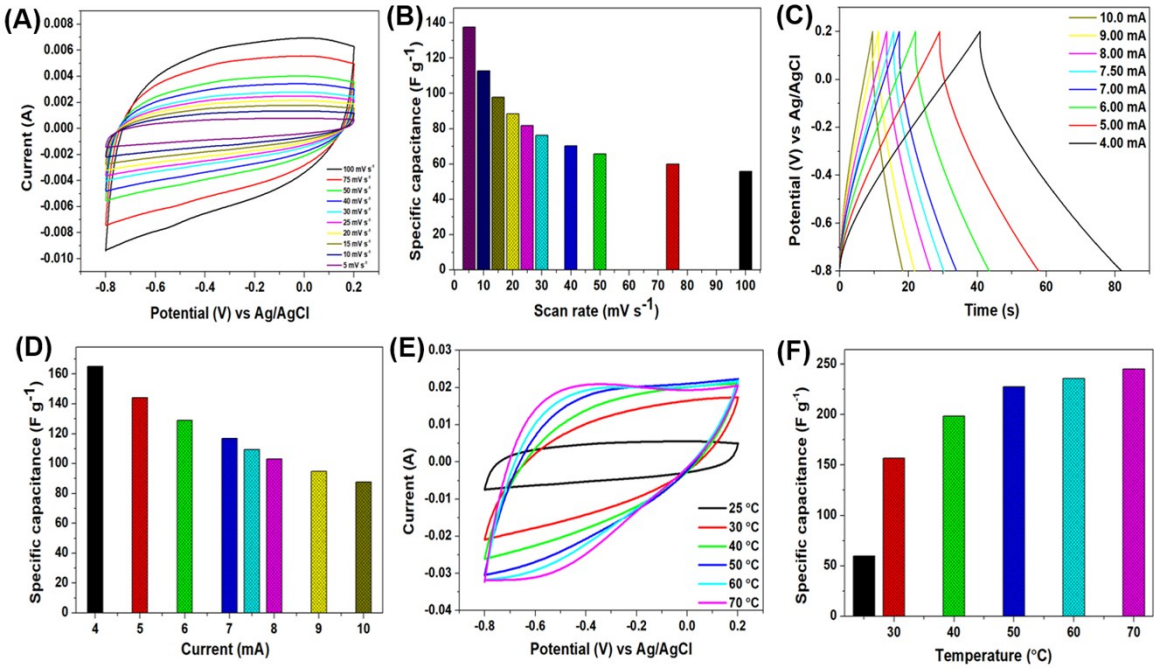

Figure S10. Electrochemical performance of as prepared rGO electrode in three electrode system. (A) Cyclic voltammetric profile of rGO electrode measured at various scan rates (5 to100 mV s^{-1}), (B) effect of scan rate on the specific capacitance of rGO electrode, (C) Galvanostatic charge-discharge profile of rGO electrode measured at different current (4 to 10 mA), (D) effect of current on specific capacitance of rGO electrode, (E) cyclic voltammetric profile of rGO electrode measured at various operating temperature, and (F) effect of temperature on specific capacitance of rGO electrode from cyclic voltammetric profile.

Table S1. The summary of electrochemical performances of Cu_2MoS_4 and Cu_2MoS_4-rGO electrode and reported electrodes for supercapacitor application using three-electrode configurations.

Material	Preparation method	Specific capacitance (F g^{-1})	Reference
CuO	Wet chemical method	88.5	[1]
RuO_2	Chemical synthesis	50	[2]
MoO_3	Solution combustion method	108.88	[3]
MoS_2	Hydrothermal	92.85	[4]
CuS	Sonochemically	62.77	[5]
ZnS	Solvothermal	32.8	[6]
WS_2	Chemical exfoliation	40	[7]
$CuSbS_2$	Colloidal method	22	[8]
$CuSbSe_2$	Colloidal method	34	[8]
Cu_2MoS_4	**Hydrothermal**	**135.78**	**This work**
Cu_2MoS_4-rGO	**Hydrothermal**	**231.51**	**This work**

Table S2. The summary of EIS parameters of Cu_2MoS_4-rGO electrode at different operating temperatures.

Temperature (°C)	**Solution resistance (R_s, Ω)**	**charge transfer resistance (R_{ct}, Ω)**	**Bode phase angle (°)**
25 °C	1.90	3	57.08
30 °C	1.51	2.96	61.91
40 °C	1.38	2.89	61.64
50 °C	1.16	2.1	63.53
60 °C	1.08	1.9	64.77
70 °C	1.01	1.8	65.36
80 °C	0.92	1.6	66.23

Notes and references

1 Y. X. Zhang, M. Huang, F. Li and Z. Q. Wen, *Int. J. Electrochem. Sci*, 2013, **8**, 8645–8661.

2 V. D. Patake and C. D. Lokhande, *Appl. Surf. Sci.*, 2008, **254**, 2820–2824.

3 G. P. Nagabhushana, D. Samrat and G. T. Chandrappa, *RSC Adv.*, 2014, **4**, 56784–56790.

4 K. Krishnamoorthy, G. K. Veerasubramani, S. Radhakrishnan and S. J. Kim, *Mater. Res. Bull.*, 2014, **50**, 499–502.

5 K. Krishnamoorthy, G. K. Veerasubramani, S. Radhakrishnan and S. J. Kim, *J. Nanosci. Nanotechnol.*, 2015, **15**, 4409–4413.

6 R. Ramachandran, M. Saranya, P. Kollu, B. P. C. Raghupathy, S. K. Jeong and A. N. Grace, *Electrochim. Acta*, 2015, **178**, 647–657.

7 C. C. Mayorga-Martinez, A. Ambrosi, A. Y. S. Eng, Z. Sofer and M. Pumera, *Electrochem. commun.*, 2015, **56**, 24–28.

8 K. Ramasamy, R. K. Gupta, S. Palchoudhury, S. Ivanov and A. Gupta, *Chem. Mater.*, 2014, **27**, 379–386.